Magnetic phase diagram of the half-filled three-dimensional Hubbard model

Kok-Kwei Pan
Physics Group, Department of General Studies, Chang Gung College of Medicine and Technology, No. 259, Wen-Hua 1st Road, Kwei-San, Tao-Yuan, Taiwan, Republic of China

Yung-Li Wang
Department of Physics, Florida State University, Tallahassee, Florida 32306
(Received 15 July 1996; revised manuscript received 18 October 1996)

Magnetic properties of the half-filled Hubbard model on three-dimensional bipartite lattices have been studied by using the linked-cluster series expansion method. The series for the free energy and the staggered susceptibility have been calculated as a function of βt for three-dimensional bipartite lattices for an arbitrary value of the Coulomb interaction U. We obtain a transition from a paramagnetic to an antiferromagnetic $U/t-T_N/t$ phase diagram from the divergence of the staggered susceptibility series. Comparisons with Monte Carlo simulation, Onsager reaction field result of an effective spin Hamiltonian, and large-U Heisenberg high-temperature solutions are made. [S0163-1829(97)09205-9]

I. INTRODUCTION

The Hubbard model[1] is one of the simplest models which describes the behavior of correlated electron systems. It has long been used in describing the metal-insulator transition,[2] antiferromagnetism,[3] and ferromagnetism.[4] Most recently, the Hubbard model has also been proposed[5] to study the physical mechanism of high-temperature superconductivity.

The Hamiltonian of the single-band Hubbard model is given by

$$H=U\sum_i n_{i\uparrow}n_{i\downarrow}-\sum_{i,\sigma}\mu_{i\sigma}n_{i\sigma}+t\sum_{\langle i,j\rangle,\sigma}(c^+_{i\sigma}c_{j\sigma}+c^+_{j\sigma}c_{i\sigma}), \tag{1}$$

where U is the on-site Coulomb repulsion potential, t is the nearest-neighbor hopping integral, $c^+_{i\sigma}$, $c_{i\sigma}$ are creation, annihilation operators for localized electron states of spin σ on site i, and $n_{i\sigma}=c^+_{i\sigma}c_{i\sigma}$. The site-dependent effective chemical potential $\mu_{i\sigma}$ includes a uniform magnetic field h and a staggered magnetic field g,

$$\mu_{i\sigma}=\mu+\alpha(\sigma)(h\pm g), \tag{2}$$

where the sign ±1 depends on whether the ith site belongs to the A or B sublattice and $\alpha(\sigma)$ is $+1$ and -1 for spin $\sigma=\uparrow$ and $\downarrow$, respectively.

Despite the simplicity of the model, no exact solutions exist except in one dimension.[6] In more than one dimension, the model is not exactly solvable. A variety of approximate methods have been used to study this problem. These include mean-field theory,[7] random phase approximation,[8] series expansion method,[9–13] Onsager reaction field approach of an effective spin Hamiltonian,[14] functional integral technique,[15,16] quantum Monte Carlo simulations,[17,18] and exact diagonalization.[19] Despite these efforts the ground state or the thermodynamics of the Hubbard model are not fully known.

Series expansion method has provided the most accurate results in the study of phase transition and critical phenomena in spin systems.[25] However, the method has not been widely used to study the correlated electrons systems. In this paper we study the antiferromagnetic phase of the half-filled Hubbard model for the simple cubic lattice and the body-centered cubic lattice using the linked-cluster series expansion method. The linked cluster expansion method has been the most efficient theoretical method for solving many-body problems. This method has been extensively used on spin systems with crystalline potentials involved.[20] The method sums up all perturbation terms to certain order and estimates the result through a well-developed extrapolation method. The calculation of the thermodynamic properties using this method covers the whole range of temperature, above as well as below the critical temperature. Above the critical temperature the linked cluster series are identical to the high-temperature series.

Recently, we developed a generalized linked-cluster expansion technique[13] with the multiple-site Wick reduction theorem applied to the Hubbard model. We generate the series expansion of the grand potential and the staggered magnetic susceptibility of the Hubbard model by the generalized linked-cluster expansion method. We have obtained the first five terms of the grand potential and the staggered susceptibility series. In the strong-coupling limit $U/t\rightarrow\infty$, our staggered susceptibility series are identical to the high-temperature series expansions (HTSE's) of spin-1/2 antiferromagnetic Heisenberg model. The resultant Néel temperature T_N as a function of U/t is in broad agreement with the Onsager reaction field calculations.

The paper is organized as follows. In Sec. II we discuss briefly the generalized linked-cluster series expansion of the grand potential for the Hubbard model. We have developed a general computer program written in the programming language *Fortran* to perform all calculations symbolically. In Sec. III we give the result of an analysis of the series and present the resulting magnetic phase diagram of the half-filled Hubbard model. A comparison with related work is also presented. Finally, a summary is given in Sec. IV.

II. GENERALIZED LINKED-CLUSTER EXPANSION

The Hubbard Hamiltonian (1) is split into two parts

$$H = H_0 + H_1 . \tag{3}$$

H_0 is the unperturbed single-site Hamiltonian of the diagonal form

$$H_0 = U\sum_i n_{i\uparrow} n_{i\downarrow} - \mu \sum_i (n_{i\uparrow} + n_{i\downarrow}) - g\sum_i (n_{i\uparrow} - n_{i\downarrow}) + g\sum_j (n_{j\uparrow} - n_{j\downarrow}), \tag{4}$$

where i and j refer to the sites of two distinct interpenetrating sublattices and g is the staggered magnetic field for calculating the staggered susceptibility.

The perturbation part H_1 contains only the hopping term

$$H_1 = \sum_{\langle i,j\rangle,\sigma} t_{i,j}(c^+_{i\sigma} c_{j\sigma} + c^+_{j\sigma} c_{i\sigma}). \tag{5}$$

The grand potential F of the Hubbard model can be written as

$$F = F_0 + \Delta F, \tag{6}$$

where F_0 is the grand potential corresponding to the unperturbed Hamiltonian H_0 and ΔF is expressed as[21]

$$\Delta F = -\frac{1}{\beta}\sum_{n=1}^{\infty} \frac{(-1)^n}{n!} \int_0^\beta d\tau_1 \int_0^\beta d\tau_2 \cdots \int_0^\beta d\tau_n \times \langle T_\tau [H_1(\tau_1) H_1(\tau_2) \cdots H_1(\tau_n)]\rangle_c , \tag{7}$$

where $\beta = (k_B T)^{-1}$ and the subscript c means the cumulant part of the τ-ordered products, or, in the diagram analysis, linked graphs only are considered.

It is convenient to represent the terms in the series expansion by diagrams. Diagrams involving up to eight interaction lines are shown in Table I, where each $H_1(\tau)$ in the grand potential expansion corresponds to the nearest-neighbor pairs of annihilation and creation operators which represent the hopping processes over the entire lattice. Each pair of factors, $t_{ij} c^+_{i\sigma} c_{j\sigma}$, is represented by an arrow from site j to the nearest-neighbor site i.

A product of $\hat{H}_1(\tau)$ in the grand potential expansion is represented by graphs which are composed of directed arrows. The expansion of ΔF then can be expressed as

$$\Delta F = -\frac{1}{\beta}\sum_{n,g_n}^{\infty} \frac{(-1)^n}{n!} W(g_n) L(g_n) I(g_n). \tag{8}$$

The summation is over all linked (connected) graphs where g_n indicates an nth-order linked graph. $W(g_n)$ is the weight of the graph or the number of topologically equivalent graphs appearing in the expansion. $L(g_n)$ is the *lattice constant* of the graph. $I(g_n)$ is the value of the τ integral of the cumulant product which the graph represents. The graphs and the weights of the graphs in Table I are produced from the Ising graphs by an algorithm which has been implemented on a computer. Summation over the lattice sites is obtained by taking the appropriate free multiplicity as the lattice constant[22] and multiplying the term by t^n. The free multiplicity can be expressed in terms of weak embedded lattice constants.[23] The nonzero lattice constants in terms of weak embedded lattice constants for the bipartite graphs are shown in Table II.

Each diagram represents a term in the expansion of $-\beta\Delta F$. The first step in the calculation of the τ integrals implied by each graph is to express the cumulants or the semi-invariants in terms of moments or thermal averages. We use Eq. (9) to transform the cumulants to the moments,[24] where $\langle [O_1 O_2 \cdots O_n]\rangle_c$ represents the cumulant of the product of fermion operators:

TABLE I. List of free-energy connected graphs.

Graph	Weight	Lattice Constant	Graph	Weight	Lattice Constant
	1	LC(1)		20160	LC(4)
	3	LC(1)		20160	LC(4)
	12	LC(2)		1680	LC(4)
	6	LC(5)			
	10	LC(1)		10080	LC(6)
	180	LC(2)		40320	LC(6)
	120	LC(3)		20160	LC(6)
	360	LC(3)		5040	LC(8)
	360	LC(5)			
	720	LC(6)		20160	LC(8)
	120	LC(7)		40320	LC(10)
	35	LC(1)		20160	LC(10)
	1120	LC(2)		20160	LC(10)
	1260	LC(2)		40320	LC(10)
	10080	LC(3)		10080	LC(9)
	5040	LC(3)		20160	LC(9)
	5040	LC(3)		20160	LC(13)
	3360	LC(5)		20160	LC(7)
	10080	LC(5)		40320	LC(12)
	5040	LC(5)		5040	LC(11)
	630	LC(5)		5040	LC(14)
	5040	LC(5)			

TABLE II. The nonzero lattice constants (LC) in terms of weak embedded lattice constants for the bipartite graphs.

LC number	LC in terms of weak embedded lattice constants
LC(1)	z
LC(2)	z^2
LC(3)	z^3
LC(4)	z^4
LC(5)	$8p_4+2z^2-z$
LC(6)	$8zp_4+2z^3-z^2$
LC(7)	$12p_6-48p_4+48zp_4+5z^3-6z^2+2z$
LC(8)	$12p_{6A}+24p_4+z^3+z^2-z$
LC(9)	$(8p_4+2z^2-z)^2/z$
LC(10)	$z^2(8p_4+2z^2-z)$
LC(11)	$48p_{8R}+72p_{6A}+56p_4+z^4+z^2-z$
LC(12)	$z(12p_6-48p_4+48zp_4+5z^3-6z^2+2z)$
LC(13)	$(8p_4+2z^2-z)^2$
LC(14)	$16p_{223}-96p_{8R}+336p_{6A}-96p_6+96zp_6+264p_4+256{p_4}^2$ $-448zp_4+224p_4z^2-768p4^2/z+14z^4-28z^3+20z^2-5z$

$$\langle T_\tau[O_1(\tau_1)O_2(\tau_2)\cdots O_n(\tau_n)]\rangle_c = \sum_{l=1}^{n}(l-1)!(-1)^{l-1}(-1)^{P_l} \times \sum_{p(n,l)}\left\langle T_\tau\left[\prod_{j=1}^{m_1}O_j(\tau_j)\right]\right\rangle_0\cdots\left\langle T_\tau\left[\prod_{q=1}^{m_k}O_q(\tau_q)\right]\right\rangle_0, \tag{9}$$

$p(n,l)$ represents a partition of n operators $O_1, O_2,\ldots,O_n$ into l sets without regard to the order, P_l is the number of interchanges of the fermion operators for this arrangement, and $m_1,m_2,\ldots,m_n$ represents the number of operators in each set. A program has been developed to calculate this transformation.

Next the fermion operators in each product are replaced by standard basis operators.[13] The replacement of the product of fermion operators by standard basis operators in the thermal average expression is also done by a computer program. All nonzero contributions are found and regrouped with terms of the same τ by the program. Since the standard basis operators include pseudofermion operators, the sign of each expression is calculated when these operators are interchanged.

Finally, the integrals containing a product of standard basis operators are calculated by using the multiple-site Wick reduction theorem[20,13]

$$\int_0^\beta d\tau_1\cdots\int_0^\beta d\tau_k\cdots\int_0^\beta d\tau_n\langle T_\tau[I_1(\tau_1)\cdots I_k(\tau_k)\cdots I_n(\tau_n)]\rangle_0 = \frac{1}{\epsilon_k}\int_0^\beta d\tau_1\cdots\int_0^\beta d\tau_n[\langle T_\tau\{[I_1,I_k]_{\tau_1}\cdots I_n(\tau_n)\}\rangle_0+\langle T_\tau\{I_1(\tau_1)[I_2,I_k]_{\tau_2}\cdots I_n(\tau_n)\}\rangle_0+\cdots+\langle T_\tau\{I_1(\tau_1)\cdots[I_n,I_k]_{\tau_n}\}\rangle_0]. \tag{10}$$

The operator I_k is a product of even number of pseudofermion operators or a product of pseudospin operators or a product of a mixture of these operators. The pseudospin operators commute and pseudofermion operators anticommute under the symbol of the τ product. The mixture of τ-dependent standard basis operators integral can be calculated by successive application of the Wick reduction integral formula. τ-independent standard basis operators integral are calculated by forming all permutations of standard basis operators. A general computer program has been developed to perform τ-dependent integral as well as τ-independent integral calculation symbolically.

We calculate the grand potential F by the method described above. The resulting expression can be written as

$$\beta F=\beta F_0+\sum_{n=2}^{\infty} f_n(\beta U,\beta\mu,\beta g)(\beta t)^n. \tag{11}$$

The staggered susceptibility is calculated from the grand potential by differentiation. We consider the case of half-filling, where the chemical potential is $\mu=U/2$. The zero-field staggered susceptibility at half-filling is given as

$$\chi^s = -\beta \left. \frac{\partial^2(\beta F)}{\partial(\beta g)^2} \right|_{g=0} = \beta\chi_0^s + \beta \sum_{n=2}^{\infty} a_n(\beta U, \eta)(\beta t)^n, \tag{12}$$

where

$$\eta = \frac{\exp(\beta U/2)}{2[1+\exp(\beta U/2)]}. \tag{13}$$

The coefficients a_n for χ^s and f_n for F are expressed as polynomials in the variables $(\beta U)^{-1}$, $\exp(-\beta U)$, and η. The coefficients a_n and f_n up to eighth order for the bipartite lattice are available upon request.

The series obtained have been checked (i) in the $U=0$ limit and (ii) in the strong-coupling limit $U/t \to \infty$ at half-filling. In the noninteracting case ($U=0$), the Hamiltonian becomes trivial, and the single-particle eigenstates have energies

$$\epsilon_{\mathbf{k}} = tz\Gamma_{\mathbf{k}}, \quad \text{where } \Gamma_{\mathbf{k}} = \frac{1}{z}\sum_{\delta} e^{i\mathbf{k}\cdot\delta}, \tag{14}$$

z is the number of nearest neighbors, and δ is a nearest-neighbor vector. The zero field grand potential F of noninteracting fermions is

$$F = -\frac{2}{\beta}\sum_{\mathbf{k}} \ln\{1+\exp[\beta(\mu-\epsilon_{\mathbf{k}})]\}. \tag{15}$$

Expanding around $\beta\epsilon_{\mathbf{k}}=0$, one obtains the expansion

$$\beta F = \beta F_0 + F_2(\beta t)^2 + F_4(\beta t)^4 + F_6(\beta t)^6 + F_8(\beta t)^8 + \cdots. \tag{16}$$

The polynomials F_n are given as

$$F_0 = -\frac{2}{\beta}\ln[1+\exp(\beta\mu)], \tag{17}$$

$$F_2 = -[\gamma]\frac{z^2}{N}\sum_{\mathbf{k}}\Gamma_{\mathbf{k}}^2,$$

$$F_4 = -\frac{1}{12}[\gamma - 6\gamma^2]\frac{z^4}{N}\sum_{\mathbf{k}}\Gamma_{\mathbf{k}}^4,$$

$$F_6 = -\frac{1}{360}[\gamma - 30\gamma^2 + 120\gamma^3]\frac{z^6}{N}\sum_{\mathbf{k}}\Gamma_{\mathbf{k}}^6,$$

$$F_8 = -\frac{1}{20160}[\gamma - 126\gamma^2 + 1680\gamma^3 - 5040\gamma^4]\frac{z^8}{N}\sum_{\mathbf{k}}\Gamma_{\mathbf{k}}^8,$$

where $\gamma = \exp(\beta\mu)/[1+\exp(\beta\mu)]^2$. In the case of nearest-neighbor interaction, the lattice sums in terms of weak embedded lattice constants for bipartite lattices (simple cubic, body-centered cubic) are given as

$$\frac{z^2}{N}\sum_{\mathbf{k}}\Gamma_{\mathbf{k}}^2 = z,$$

$$\frac{z^4}{N}\sum_{\mathbf{k}}\Gamma_{\mathbf{k}}^4 = 8p_4 + 2z^2 - z, \tag{18}$$

$$\frac{z^6}{N}\sum_{\mathbf{k}}\Gamma_{\mathbf{k}}^6 = 12p_6 - 48p_4 + 48zp_4 + 5z^3 - 6z^2 + 2z,$$

$$\begin{aligned}\frac{z^8}{N}\sum_{\mathbf{k}}\Gamma_{\mathbf{k}}^8 = {} & 16p_{223} - 96p_{8R} + 336p_{6A} - 96p_6 + 96zp_6 + 264p_4 \\ & + 256p_4^2 - 448zp_4 + 224p_4z^2 - 768p4^2/z + 14z^4 \\ & - 28z^3 + 20z^2 - 5z.\end{aligned}$$

In the $U=0$ limit, our results agree completely with the exact solution given above.

At half-filling and in the strong-coupling limit $U/t \to \infty$, our staggered susceptibility $\chi^s(g=0)$ series are identical to the high-temperature series expansions of the antiferromagnetic Heisenberg model.[25,26] Furthermore, the series obtained from different graphs can also be checked internally. The grand potential or the staggered susceptibility series of a graph is invariant under an interchange of up-spin fermion operator and down-spin fermion operator in zero magnetic field. Therefore a symmetric pair of graphs obtained by interchanging of up-spin and down-spin yield the same result in zero magnetic field. In this way all symmetric pairs of graphs that appeared in the sixth order and the eighth order are checked.

We give the full expression for the staggered susceptibility per site at half filling, for the simple cubic lattice, and up to the $(\beta t)^8$ terms:

$$\begin{aligned}\beta^{-1}\chi^s = 1 & + \left[6 - \frac{24}{\beta U} + \frac{24}{(\beta U)^2}\right]\frac{(\beta t)^2}{(\beta U)} + \left[28 - \frac{210}{\beta U} - \frac{48}{(\beta U)^2} + \frac{1128}{(\beta U)^3}\right]\frac{(\beta t)^4}{(\beta U)^2} \\ & + \left[120 - \frac{1696}{\beta U} + \frac{3339}{(\beta U)^2} - \frac{12216}{(\beta U)^3} + \frac{77610}{(\beta U)^4}\right]\frac{(\beta t)^6}{(\beta U)^3} \\ & + \left[494.80 - \frac{10786.0}{\beta U} + \frac{54132.0}{(\beta U)^2} - \frac{169038.75}{(\beta U)^3} + \frac{10030.50}{(\beta U)^4} + \frac{4259316.80}{(\beta U)^5}\right]\frac{(\beta t)^8}{(\beta U)^4}.\end{aligned} \tag{19}$$

Since the terms that contain the exponential of $-\beta U$ are always exponentially smaller than other terms in the expression, we neglect these terms in this expression.

Similarly, the staggered susceptibility series per site at half filling for the body-centered cubic lattice is given as

$$\beta^{-1}\chi^s = 1 + \left[8 - \frac{32}{\beta U} + \frac{32}{(\beta U)^2}\right]\frac{(\beta t)^2}{(\beta U)} + \left[\frac{160}{3} - \frac{392}{\beta U} - \frac{128}{(\beta U)^2} + \frac{2208}{(\beta U)^3}\right]\frac{(\beta t)^4}{(\beta U)^2} + \left[\frac{1024}{3} - \frac{14944}{3\beta U} + \frac{11882}{(\beta U)^2} - \frac{42224}{(\beta U)^3} + \frac{224348}{(\beta U)^4}\right]\frac{(\beta t)^6}{(\beta U)^3} + \left[2073.06 - \frac{48232.02}{\beta U} + \frac{276877.30}{(\beta U)^2} - \frac{829552.25}{(\beta U)^3} - \frac{171617.02}{(\beta U)^4} + \frac{17921678.78}{(\beta U)^5}\right]\frac{(\beta t)^8}{(\beta U)^4}. \tag{20}$$

In the strong-coupling limit $U/t \to \infty$, these staggered susceptibility series are identical to the high-temperature series expansions[25,26] of the spin-1/2 antiferromagnetic Heisenberg model with nearest-neighbor coupling $J = 4t^2/U$.

III. PHASE DIAGRAM OF THE HALF-FILLED THREE-DIMENSIONAL HUBBARD MODEL

A transition from a paramagnetic to an antiferromagnetic phase diagram $(U/t - T_N/t)$ can be obtained from the divergence of the staggered susceptibility series for staggered field $g = 0$. In this work we use Padé approximants to extrapolate the staggered susceptibility series to small coupling region. The staggered susceptibility series in Eq. (19) or Eq. (20) is regarded as a series in $x = (\beta t^2)/U$:

$$\beta^{-1}\chi^s = \sum_n a_n x^n. \tag{21}$$

Padé approximants $[L/M]$ to the series expansion $\beta^{-1}\chi^s$ are defined by

$$[L/M] = \frac{n_0 + n_1 x + \cdots + n_L x^L}{1 + d_1 x + \cdots + n_M x^M}. \tag{22}$$

Since the coefficients of the power series are functions of βU, it is easy to obtain the approximants $[L/M]$ from fixed value of βU. For a given value of βU, approximants $[L/M]$ are calculated from the coefficients of $\beta^{-1}\chi^s$ series. The value of x_N at which the susceptibility diverges is estimated by finding the roots of the denominators of approximants. We have used roots from the [1/2] and [1/3] approximants. We obtain T_N/t from $T_N/t = 1/\sqrt{(x_N)(\beta U)}$ with known values of x_N and βU. We then multiply T_N/t to βU to find the corresponding value of U/t. Carrying out this procedure for different values of βU will give the $(U/t - T_N/t)$ phase diagram.

In Fig. 1 we show the $(U/t - T_N/t)$ phase diagram obtained from linked-cluster series expansion method (LCE) for the simple cubic lattice. They are plotted as a solid line which was estimated from the average of the [1/2] and [1/3] approximants with error bars. The error bars are estimated as half the spread of these approximants. Figure 1 also compares our results with T_N of the three-dimensional (3D) Hubbard model obtained from Onsager reaction field (ORF) calculations of an effective Heisenberg Hamiltonian by Szczech *et al.*[14] We see that both calculations are in good agreement with each other at large U $(U/t \geq 10)$. In the strong-coupling region, both calculations approach from above the strong-coupling Heisenberg estimate of $T_N = 3.83t^2/U$ obtained from high-temperature series calculations.[25,26] We also show the results of quantum Monte Carlo[17] calculations which yield the molecular field result $T_N = 6t^2/U$ in the strong-coupling limit and the conjectured form for the true $T_N(U)$ by Kakehasi and Hasegawa.[16]

In the intermediate coupling region, the Néel temperature in the linked-cluster series expansion is lower than that in the ORF calculation. We believe this to be the effects of couplings beyond nearest-neighbor which stabilize the antiferromagnetic phase in the ORF (Ref. 14) calculation. However, the convergence of linked-cluster series expansion is also slow in this region. Since the series extrapolation is better at large U, and not so well as small U, it is important to obtain the higher-order terms to describe more correctly the behavior of $(U/t - T_N/t)$ phase diagram in the weak-coupling region.

We have also attempted to analyze the series using the ratio method.[25] The critical temperature is determined from the value of x_N at which χ^s diverges. We have

$$\frac{1}{x_N} = \frac{\beta_N U}{(\beta_N t)^2} = \lim_{n\to\infty} \frac{a_n}{a_{n-1}}. \tag{23}$$

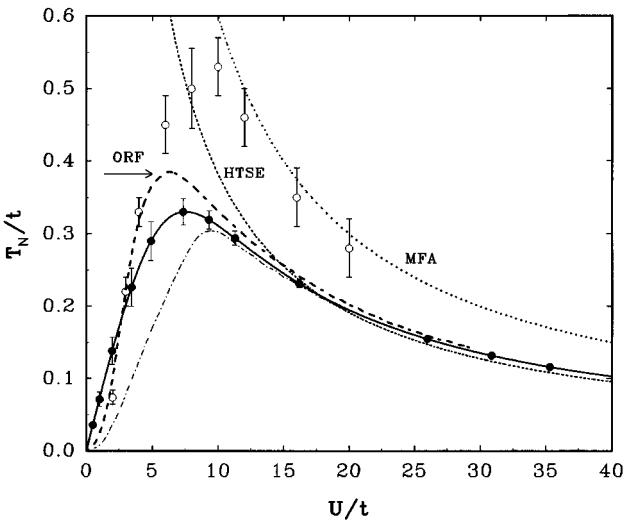

FIG. 1. The Néel temperature T_N/t as a function of U/t of the half-filled Hubbard model for the simple cubic lattice. Solid line gives results of the linked cluster series expansion. Error bars indicate spread of the Padé approximants. Dashed line gives Onsager reaction field method (ORF, Ref. 14). The open circles represent QMC results. Dotted curves show the molecular-field approximation (MFA) and high-temperature series expansion (HTSE) for the Heisenberg model. Also shown is a plausible form for T_N curve given in Ref. 16 (dot-dashed line).

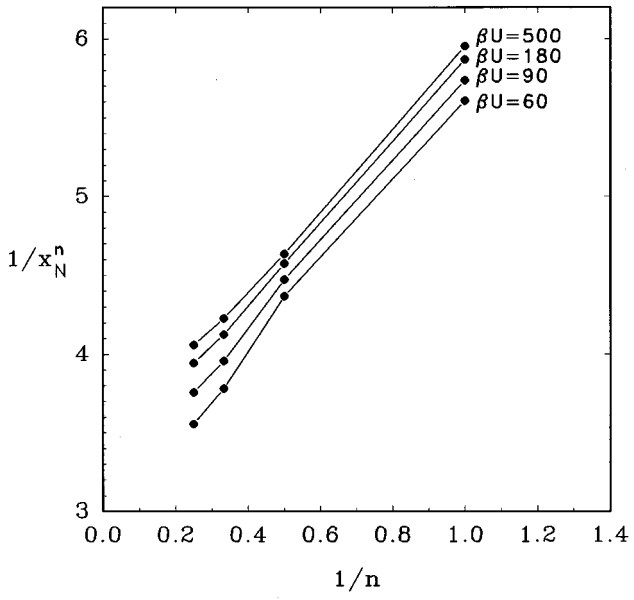

FIG. 2. The ratio of two successive coefficients of the staggered susceptibility series in the paramagnetic phase $1/x_N^n$ plotted vs $1/n$ for the simple cubic lattice with different values of βU.

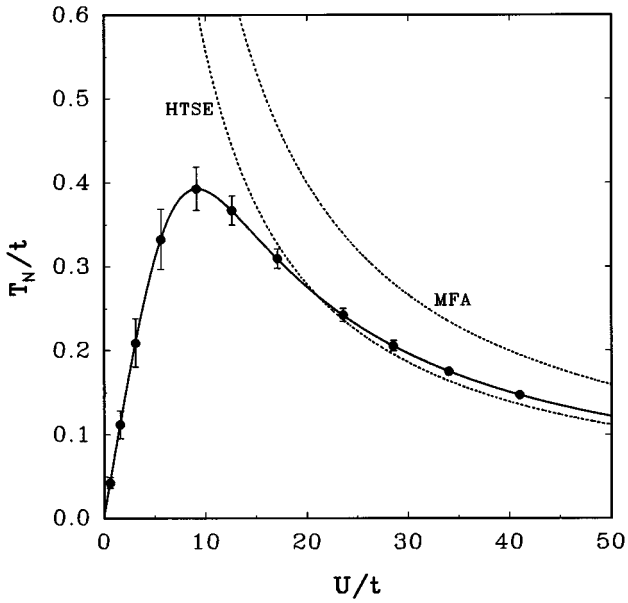

FIG. 3. The Néel temperature T_N/t as a function of U/t of the half-filled Hubbard model for the body-centered cubic lattice. Solid line gives results of the linked cluster series expansion. Error bars indicate spread of the Padé approximants. Dotted curves show the molecular-field approximation (MFA) and high-temperature series expansion (HTSE) for the Heisenberg model.

For a series with only a finite number of terms known, we can only estimate the value of x_N by extrapolation. We define

$$\frac{1}{x_N^n}=\frac{a_n(\beta U)}{a_{n-1}(\beta U)}. \tag{24}$$

For each value of βU, the critical value of x_N is estimated by extrapolation:

$$\frac{1}{x_N}=n\,\frac{a_n}{a_{n-1}}-(n-1)\,\frac{a_{n-1}}{a_{n-2}}. \tag{25}$$

T_N/t is obtained from $T_N/t=1/\sqrt{(x_N)(\beta U)}$. The corresponding value of U/t is calculated from T_N/t and βU. The $1/x_N^n$ versus $1/n$ plot for the simple cubic lattice with certain values of βU is shown in Fig. 2. For larger values of βU a straight line can be drawn through the points except the first one. However, there is still a small deviation of the points from a straight line. For the smaller value of βU, corresponding to smaller value of U/t, the oscillation grows bigger. In general, the ratio method analysis for the larger values of U/t agrees with the results obtained from the Padé approximants analysis.

Similarly, we show the $(U/t-T_N/t)$ phase diagram obtained from linked-cluster series expansion method for the bcc lattice in Fig. 3. T_N/t versus U/t curve was obtained from the average of the [1/2] and [1/3] approximants with error bars. The error bars are estimated as half the spread of these approximants. The qualitative behavior of the phase diagram is similar to the simple cubic one. The exact strong-coupling Heisenberg estimate of $T_N=5.59t^2/U$ obtained from high-temperature series calculations[25,26] and the molecular field result of $T_N=8t^2/U$ are also shown for comparison.

IV. SUMMARY

In summary, we obtained series for the grand potential and the staggered susceptibility of the half-filled Hubbard model using the linked-cluster series expansion method. A transition from a paramagnetic to an antiferromagnetic phase diagram $(U/t-T_N/t)$ for 3D bipartite lattices (simple cubic and body-centered cubic) were obtained using the series extrapolation method. The resultant Néel temperature T_N as a function of U/t for the simple cubic lattice is in broad agreement with the Onsager reaction field calculations except in the weak-coupling limit. The convergence of the series is slow in the moderate and weak-coupling region. Higher-order terms are needed to describe the correct behavior of magnetic phase boundary of the Hubbard model in the weak-coupling region. A phase diagram for the body-centered cubic lattice is also shown in the present calculation.

ACKNOWLEDGMENTS

This research was supported by the National Science Council of Republic of China under Grant No. NSC85-2112-M182-002. We would like to thank Professor Felix Lee for helpful discussions in calculating the lattice constants. The computations were done on the DEC Alpha and Convex C3840 of the National Center for High-Performance Computing (NCHC). We wish to thank NCHC for its support. We also acknowledge the National Tsing Hua University Physics Department for providing part of the computer time for the present calculation.

[1] J. Hubbard, Proc. R. Soc. London Ser. A **276**, 238 (1963); **277**, 237 (1964); **281**, 401 (1964); **285**, 542 (1965).
[2] N. F. Mott, Rev. Mod. Phys. **40**, 677 (1968); W. F. Brinkman and T. M. Rice, Phys. Rev. B **2**, 1324 (1970).
[3] P. W. Anderson, Solid State Phys. **14**, 99 (1963).
[4] Y. Nagaoka, Phys. Rev. **147**, 392 (1966).
[5] P. W. Anderson, Science **235**, 1196 (1987).
[6] E. H. Lieb and F. Y. Wu, Phys. Rev. Lett. **20**, 1445 (1968).
[7] D. Penn, Phys. Rev. **142**, 350 (1966).
[8] S. Doniach and E. Sondheimer, *Green's Functions for Solid State Physicists* (Benjamin, Reading, MA, 1982); J. R. Schrieffer, X. G. Wen, and S. C. Zhang, Phys. Rev. B **39**, 11 663 (1989).
[9] D. F. B. ten Haaf, P. W. Brouwer, P. J. H. Denteneer, and J. M. J. van Leeuwen, Phys. Rev. B **51**, 353 (1995); D. F. B. ten Haaf and J. M. J. van Leeuwen, *ibid*. **46**, 6313 (1992).
[10] J. A. Henderson, J. Oitmaa, and M. C. B. Ashley, Phys. Rev. B **46**, 6328 (1992).
[11] K. Kubo, Prog. Theor. Phys. **64**, 758 (1980); K. Kubo and M. Tada, *ibid*. **69**, 1345 (1983); **71**, 479 (1984).
[12] Y. S. Yang, C. J. Thompson, and A. J. Guttmann, Phys. Rev. B **42**, 8431 (1990); C. J. Thompson, Y. S. Yang, A. J. Guttmann, and M. F. Sykes, J. Phys. A **24**, 1261 (1991); Y. S. Yang and C. J. Thompson, J. Phys. A **24**, L279 (1991).
[13] K. K. Pan and Y. L. Wang, Phys. Rev. B **43**, 3706 (1991); J. Appl. Phys. **69**, 4656 (1991).
[14] Y. H. Szczech, M. A. Tusch, and D. E. Logan, Phys. Rev. Lett. **74**, 2804 (1995); M. A. Tusch, Y. H. Szczech, and D. E. Logan, Phys. Rev. B **53**, 5505 (1996).
[15] Y. Kakehashi and P. Fulde, Phys. Rev. B **32**, 1595 (1985); Y. Kakehashi and J. H. Samson, *ibid*. **33**, 298 (1986).
[16] Y. Kakehashi and H. Hasegawa, Phys. Rev. B **36**, 4066 (1987); **37**, 7777 (1988).
[17] R. T. Scalettar, D. J. Scalapino, R. L. Sugar, and D. Toussaint, Phys. Rev. B **39**, 4711 (1989).
[18] J. E. Hirsch and S. Tang, Phys. Rev. Lett. **62**, 591 (1989); S. R. White, D. J. Scalapino, R. L. Sugar, E. Y. Loh, J. E. Gubernatis, and R. T. Scalettar, Phys. Rev. B **40**, 506 (1989).
[19] E. Dagotto, Rev. Mod. Phys. **66**, 763 (1994), and references therein.
[20] Y. L. Wang, C. Wentworth, and B. Westwanski, Phys. Rev. B **32**, 1805 (1985); C. Wentworth and Y. L. Wang, *ibid.* **36**, 8687 (1987).
[21] A. A. Abrikosov, L. P. Gor'kov, and I. Ye. Dzyaloshinsky, *Quantum Field Theoretical Methods in Statistical Physics* (Pergamon, New York, 1965).
[22] M. Wortis, in *Phase Transitions and Critical Phenomena Vol. 3*, edited by C. Domb and M. S. Green (Academic, New York, 1974).
[23] F. Lee and H. H. Chen, Phys. Rev. B **30**, 2724 (1984).
[24] R. Kubo, J. Phys. Soc. Jpn. **17**, 1100 (1962).
[25] G. S. Rushbrooke, G. A. Baker, and P. J. Wood, in *Phase Transitions and Critical Phenomena Vol. 3*, edited by C. Domb and M. S. Green (Ref. 22).
[26] G. S. Rushbrooke and P. J. Wood, Mol. Phys. **6**, 409 (1963).